Minimum Copper Losses Per Torque Optimization on Electrically Excited Synchronous Motors for Electric Vehicles Applications

Charbel Zaghrini, Gabriel Khoury, Maurice Fadel, Ragi Ghosn, Flavia Khatounian

Minimum Copper Losses Per Torque Optimization on Electrically Excited Synchronous Motors for Electric Vehicles Applications

Charbel Zaghrini
ESIB, CINET, Faculté d'Ingénierie
Université Saint-Joseph de Beyrouth
Beirut, Lebanon
charbel.zaghrini@net.usj.edu.lb

Gabriel Khoury
ESIB, CINET, Faculté d'Ingénierie
Université Saint-Joseph de Beyrouth
Beirut, Lebanon
gabriel.khoury@usj.edu.lb

Maurice Fadel
LAPLACE, *Université de Toulouse*
CNRS, INPT, UPS
Toulouse, France
maurice.fadel@laplace.univ-tlse.fr

Ragi Ghosn
ESIB, CINET, Faculté d'Ingénierie
Université Saint-Joseph de Beyrouth
Beirut, Lebanon
ragi.ghosn@usj.edu.lb

Flavia Khatounian
ESIB, CINET, Faculté d'Ingénierie
Université Saint-Joseph de Beyrouth
Beirut, Lebanon
flavia.khatounian@usj.edu.lb

***Abstract*— Increased environmental and energy security concerns have made electric vehicles an attractive solution over the recent years. Therefore, improving their traction chain global efficiency, especially in high-speed region, became a major task in today's research. This paper investigates a novel optimization method applied on electric vehicles motorized by an Electrically Excited Synchronous Motor (EESM). The study proposes an algebraic method based on the Lagrange multiplier technique to control the motor torque efficiently while extending its speed limit using the additional degree of freedom offered by this type of machines. The reference currents are calculated offline and stored in lookup tables (LUT) using MATLAB/Simulink. The proposed method is compared to conventional Maximum Torque Per Ampere (MTPA) strategies applied on Internal Permanent Magnet Synchronous Machines (IPMSM) by maintaining the EESM excitation current constant and controlling the d-q axis currents for a likewise behavior. The optimization and speed limit extension benefits of the novel control scheme, especially in high-speed region, are emphasized via simulation results in the torque/speed domain.**

Keywords*— *Electric vehicles, EESM, optimization, Copper losses, efficient torque control.

I. Introduction

Since the significant appearance of electric traction applications, permanent magnet (PM) motors were the most widely used due to the advantages they bring compared to other machines in terms of efficiency, torque density, reliability and control ease [1]. However, PMSMs present some drawbacks like the high cost of rare-earth magnet and its limited supply, as well as the need of increased negative d-axis currents at high-speed which affect copper losses and efficiency. A good alternative for these types of machines would be the EESM which gained a lot of attention in electric traction applications and is currently used in commercial vehicles like Renault ZOE. These machines have flux regulation capabilities in both winding and field armatures, so their performance can be optimized to compete with PM machines especially at high-speed ranges [2].

Numerous d-q axis current optimization algorithms are proposed in literature for PM machines, especially on the IPMSM type that provides both electromagnetic and reluctance torque, which control scheme is the closest to a salient-pole EESM without excitation flux regulation [3]. Copper loss minimization algorithms are the most famous among these studies, aiming to find the minimum stator current that satisfies a target load torque without crossing voltage limits in high-speed region, also known as MTPA techniques. The latter optimization method is very popular amongst PM machines where many improvements can be found in literature, contrarily to EESMs which MTPA related works are not as popular as functional safety studies [4]. Some research suggests taking the PM synchronous machine parameter variations into account for a much precise control algorithm, as in [5] where a Sliding Mode Controller (SMC) is used to shift the operating point to correct the minimum stator current imprecision due to parameter variations. Whereas in [6], the Recursive Least Square (RLS) estimation method is used for the same matter but on an IPMSM. Another approach is found in [7] where the IPMSM d-q axis inductances difference is estimated using the deviation between actual and reference output power, then MTPA is used with the estimated values.

The mentioned approaches offer a precise optimized torque control, yet they don't provide a solution to high d-axis current injection in high-speed region. EESMs have the capability of functioning like an IPMSM by maintaining a constant flux excitation. They also provide an additional feature by reducing the excitation current rather than increasing the negative d-axis current, which offers an interesting solution to increased copper losses in field weakening region, thus ensuring optimal performance for a target load torque at high-speed. In [8], an energy efficient control based on copper losses minimization was implemented on an EESM for traction applications using the *fmincon* MATLAB optimization toolbox and LUTs, taking into account voltage and current limits. Results appeared to be promising on these types of machines, especially in high-speed area.

In this paper, a novel optimization control method is implemented on an EESM for traction applications, aiming to improve the speed/power performance when compared to PM machines, especially in flux weakening region. The EESM model and control structure are developed in section II. In section III, an MTPA strategy inspired from a conventional IPMSM d-q axis current minimizing control algorithm is applied on the EESM for a constant rated field current. The

enhanced copper losses optimization method denoted by minimum Copper Losses per Torque (minCLPT) is then addressed in section IV, where the Lagrangian multiplier method is used to determine the minimum of a constrained non-linear multi variable function including both armature and field winding currents. Finally, the energy efficiency and speed limits improvements are emphasized via simulation results in section V, using the EESM simulation tool presented in [9].

II. Electrically Excited Synchronous Motor Model and Control Structure

The field-oriented voltage equations of the salient pole EESM using Concordia transformation are given in (1)-(3):

$$V_d = R_s I_d + \frac{d}{dt}\Phi_d - p\Omega\Phi_q \quad (1)$$

$$V_q = R_s I_q + \frac{d}{dt}\Phi_q + p\Omega\Phi_d \quad (2)$$

$$V_f = R_f I_f + \frac{d}{dt}\Phi_f \quad (3)$$

Herein, V_d and V_q are the dq axis stator voltages and V_f the rotor voltage. R_s and R_f are the stator and rotor resistances respectively. I_d and I_q are the dq axis stator currents and I_f the rotor field coil current. The mechanical rotor shaft speed is denoted by Ω (rad/s) and p is the pair pole number. The corresponding flux equations are given as in (4)-(6) :

$$\Phi_d = L_d I_d + M I_f \quad (4)$$

$$\Phi_q = L_q I_q \quad (5)$$

$$\Phi_f = L_f I_f + M I_d \quad (6)$$

L_d and L_q are the dq axis stator inductances, L_f the rotor coil inductance, and M the stator-rotor coupling inductance.

The EESM produced electromagnetic torque is expressed as in (7):

$$T = pI_d I_q\left(L_d - L_q\right) + MpI_q I_f \quad (7)$$

The EESM overall control structure is illustrated in the block diagram of Fig. 1. The electric vehicle battery which DC bus voltage is denoted by V_{DC}, is connected to the power converters stage consisting of a three-phase inverter feeding the machine stator windings and a single-phase chopper connected to the field winding. Converters modeling technique is detailed in [9] where the average converter model is used for that matter. Whereas the machine rated values and parameters are listed in Table 1. It is important to note that the mentioned rated values in Table 1 are considered as maximum values since steady-state results are the main interest of this study.

The present work focuses on the algorithmic control unit which receives the user's torque setpoint denoted by T_{ref} and the machine rotation speed, with a task to deduce the optimal stator and rotor reference currents (I_{d_ref}, I_{d_ref}, I_{f_ref}) that would generate the best converters switching sequences, so the requested torque input is obtained with minimum copper losses. Conventional field-oriented control methods are used for current regulation along with decoupling strategies to eliminated cross couplings between armature and field current components shown in (1)-(6). The chopper acts as a buck converter and delivers a maximum voltage of $V_{f,N}$, whereas the Space Vector Modulation (SVM) technique used for inverter modeling allows a maximum voltage of $V_{DC}/\sqrt{3}$.

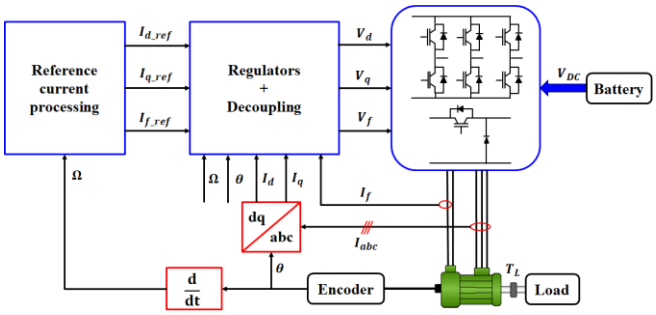

Fig. 1 Block diagram of the EESM control structure

III. Minimum Current Per Torque Strategy with Constant Excitation Flux

The goal in this section is to efficiently operate the EESM like a normal PM machine by implementing an MTPA optimization algorithm that deduces the minimum stator current while keeping the excitation current constant. This algorithm is included in the coding of the novel optimization method developed in the next section and will also serve for comparison purposes between PM machines behavior under conventional copper losses optimization methods and EESMs using their excitation current as an additional degree of freedom.

As seen in (7), EESM electromagnetic torque depends on currents I_d, I_q and I_f. There are numerous current triplets satisfying a torque-speed setpoint, thus adding the minimum current as an optimization criterion to the mathematical problem allows to find one or several combinations satisfying the given objective. However, voltage and current limits, expressed in (8)-(9), are important constraints to take into account in order to determine control algorithm limits based on the machine and power converters physical limitations.

$$V_d{}^2 + V_q{}^2 = 1.5V_{s(\max)}{}^2 \quad (8)$$

$$I_d{}^2 + I_q{}^2 = 1.5I_{s(\max)}{}^2 \quad (9)$$

Having the excitation current constant in this section, the minimum Current Per Torque (minCPT) optimization control algorithm is applied on the EESM in order to explore limitations of conventional methods and find improvements through these types of machines. The minCPT technique is very similar to MTPA and can be broken down into a simple 'objective with constraint' problem: the objective is to minimize stator currents for a $T = T_{ref}$ constraint. An effective approach to achieve this goal is the use of the Lagrangian multiplier technique developed in (11)-(13) applied to the Lagrangian equation in (10), using the objective and constraint terms affected by the Lagrange constant λ.

$$L\left(I_d, I_q\right) = I_d{}^2 + I_q{}^2 + \lambda.\left(T_{ref} - \left(pI_d I_q\left(L_d - L_q\right) + MpI_q I_f\right)\right) \quad (10)$$

$$\frac{\partial L}{\partial I_d} = 2I_d - \lambda p\left(L_d - L_q\right)I_q = 0 \quad (11)$$

$$\frac{\partial L}{\partial I_q} = \left(2 - \lambda p\left(L_d - L_q\right)\right) I_q - \lambda M p I_f = 0 \qquad (12)$$

$$\frac{\partial L}{\partial \lambda} = T_{ref} - \left(p I_d I_q \left(L_d - L_q\right) + M p I_q I_f\right) = 0 \qquad (13)$$

Using (11)-(13), a 4th order polynomial equation in I_d is obtained as shown in (14), which solution gives the minCPT optimal d-q axis current references. Fig. 2 shows the latter versus the electromagnetic torque at a rated field current.

$$p^2(L_d - L_q)^2 {I_d}^4 + 2Mp^2\left(L_d - L_q\right) I_f {I_d}^3 + 3\left(M p I_f\right)^2 {I_d}^2 + \frac{p^2 (M I_f)^3}{L_d - L_q} I_d - {T_{ref}}^2 = 0 \qquad (14)$$

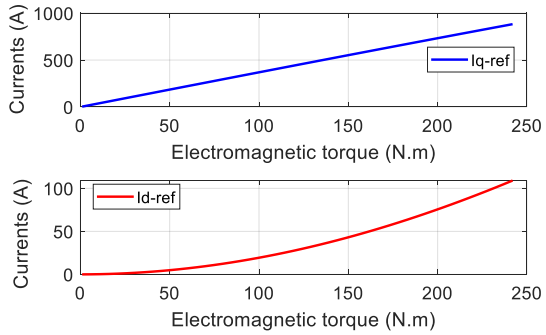

Fig. 2 minCPT optimal d-q axis current references for a constant rated field current

Having computed the optimal reference currents for minimum stator copper losses at constant rated field current, the minCPT trajectory can be plotted in the I_d - I_q plane along with constant torque contours, voltage limit ellipses and current limit circle as shown in Fig. 3. These types of machines are built in a way that voltage limit ellipses center is located outside the armature current limit circumference for a rated field current. This would limit conventional optimization methods without field current regulation at high-speed, since reaching beyond 10000 rpm would require negative d-axis currents as seen in Fig. 3.

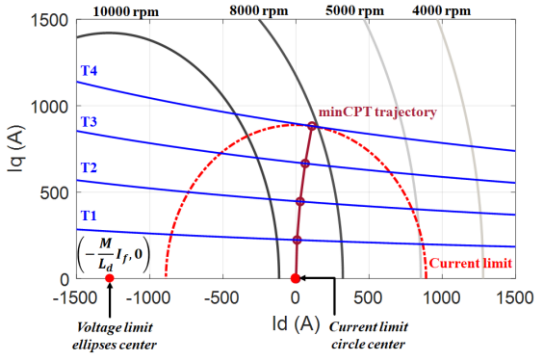

Fig. 3 Constant torque contours, voltage limit ellipses, current limit circle and minCPT trajectory in the I_d - I_q plane at rated field current

For clearer visualization, the minCPT speed limit trajectory is plotted in the torque – speed domain as shown in Fig. 4, by taking into account voltage limits in (8) for each torque value. Current limits using this strategy are respected as long as the rated torque T_N is not exceeded. The machine rated mechanical power limit P_N is also plotted in Fig. 4. Results show that conventional MTPA strategies could drive the machine to a maximum of 2.5 times the rated speed without reaching voltage limit. However, increasing the speed for a certain torque setpoint would require the migration to a flux-weakening algorithm where negative d-axis current references come into play as concluded from Fig. 3, thus increasing stator current magnitude. The flux-weakening algorithm limit curve defined by reaching both voltage and current limits, can be calculated by solving a system consisting of voltage equations shown in (1) and (2) while taking high speed and steady-state considerations, along with voltage and current limits defined in (8) and (9). The flux-weakening limit trajectory is added to the minCPT speed limit one in the torque – speed domain in Fig. 4.

As long as operating points are chosen inside the red area, the machine can normally be driven by minCPT algorithm and operating points are reached with minimum stator current without crossing voltage and current limits, thus reducing stator windings copper losses and driving the machine efficiently. Yet, the energy efficient minCPT algorithm is discarded when operating points are chosen inside the black area, as voltage limits are reached. Current magnitude is therefore increased bringing negative d-axis current into play, thus increasing copper losses. Operating points in both regions are taken as examples in Fig. 5, so that current references along with respective copper losses are clearly visualized. The latter losses are expressed as in (15):

$$P_{Co} = R_s\left({I_d}^2 + {I_q}^2\right) + R_f {I_f}^2 \qquad (15)$$

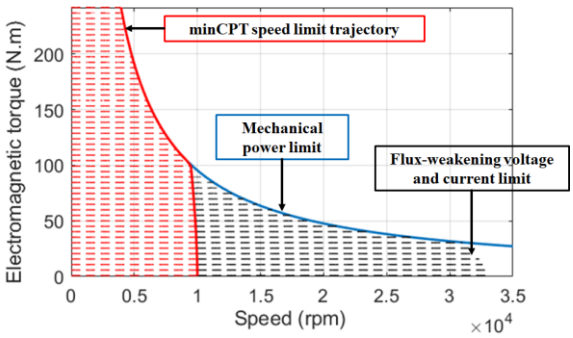

Fig. 4 minCPT and flux-weakening algorithms limit trajectories in the torque – speed domain for a rated field current

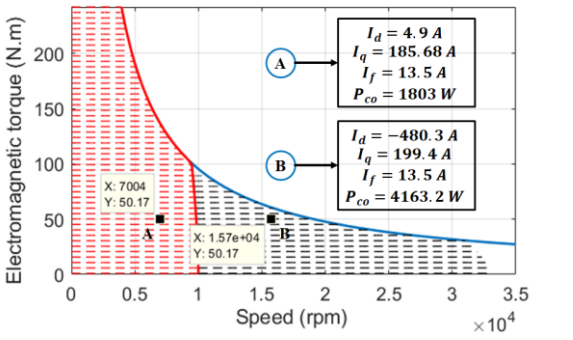

Fig. 5 Reference currents and copper losses results of operating points in both minCPT and flux weakening areas

Operating points in Fig. 5 were chosen for the same torque setpoint of 50 N.m, at speed references achieved using minCPT algorithm on one side (A at 4000 rpm), and flux-weakening algorithm on the other side (B at 15700 rpm). It is

clearly noticeable that conventional MTPA limit extension could bring many benefits to the optimization scheme since copper losses are considerable in flux-weakening region. This might be harder in the permanent magnet case where the flux is constant and cannot be implemented in the control algorithm.

IV. Minimum Copper Losses per Torque Optimization Control Algorithm

After having clearly defined the conventional PMSM copper losses algorithms, the EESMs excitation current is included in the control algorithm to extend the study for high-speed regions where flux-weakening algorithms can be costly to the drive train efficiency. The novel minCLPT optimization method consists in finding the optimal current triplets I_d, I_q, I_f that minimize the overall machine copper losses shown in (16) while achieving the user's torque setpoint. Minimum copper losses are obtained with minimum field current references, resulting potentially in machine efficiency improvement and speed limit extension. The problem can be solved by minimizing (16) using the Lagrangian multiplier method, thus solving the system of equations in (17)-(20).

$$L(I_d, I_q, I_f) = R_s({I_d}^2 + {I_q}^2) + R_r {I_f}^2 + \lambda.(T_{ref} - (pI_dI_q(L_d - L_q) + MpI_qI_f) \quad (16)$$

$$\frac{\partial L}{\partial I_d} = 2R_sI_d - \lambda p(L_d - L_q)I_q = 0 \quad (17)$$

$$\frac{\partial L}{\partial I_q} = \left(2R_s - \lambda p(L_d - L_q)\right) I_q - \lambda MpI_f = 0 \quad (18)$$

$$\frac{\partial L}{\partial I_f} = 2R_fI_f - \lambda MpI_q = 0 \quad (19)$$

$$\frac{\partial L}{\partial \lambda} = T_{ref} - (pI_dI_q(L_d - L_q) + MpI_qI_f) = 0 \quad (20)$$

The algebraic current references solution of the above equations can be obtained using MATLAB, thus have the attribute of being implemented on a Digital Signal Processor (DSP) for an online optimization scheme rather than offline LUT storage. Taking into account the machine parameter variations and magnetic saturation in the control algorithm would obviously make solutions much harder and time consuming for an online DSP implementation. This matter will be explored in future works where the optimization method will be implemented on an experimental setup. For the time being, simulation results of offline LUT current reference storage of the above equations solutions are explored and compared to conventional MTPA strategies developed in the above section. The minCLPT resulting optimal reference currents are shown in Fig. 6.

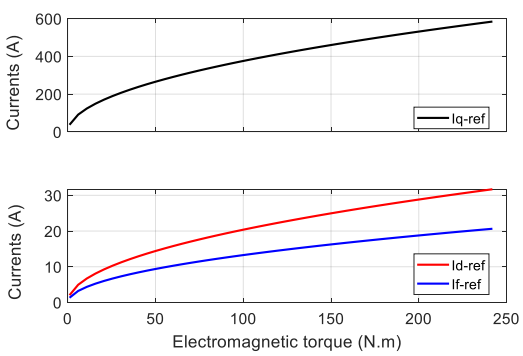

Fig. 6 minCLPT optimal reference currents

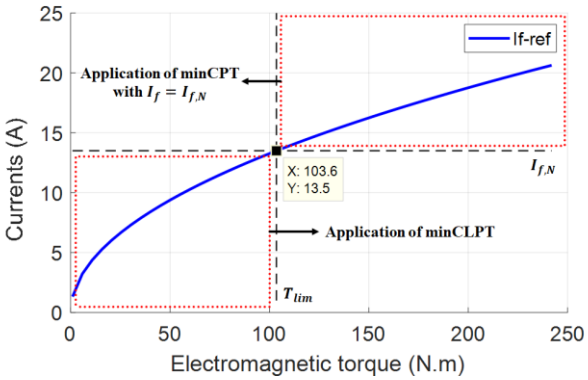

Fig. 7 minCLPT and minCPT zones of application

It is important to note that driving the machine using minCLPT algorithm alone is not possible since the calculated reference field current reaches its rated value at a certain torque limit denoted by T_{lim} in Fig. 7, where the reference field current is plotted versus the electromagnetic torque along with minCPT and minCLPT operating areas. It is important to switch back to the minCPT algorithm developed in previous section when T_{lim} is reached and thus operate the machine under minimal stator currents at a constant rated field current. This would not be considered as a major drawback for the optimization method as the main interest consists in increasing speed limit along with energy efficiency benefits, and most high-speed requirements are usually found in low to mid torque regions rather than high torque areas where power limit are usually reached.

Comparing minCLPT current references results in Fig. 6 to the minCPT ones in Fig. 2, shows that the field current inclusion in the control algorithm brings some sort of relief to the d-axis current where the reference torque is achieved with lower values for both I_d and I_f which should bring benefits not only to stator and rotor copper losses but also to speed limits that should potentially extend with lower field current values. The speed limit extension benefits are explored through Fig. 8, where the minCLPT speed limit extension defined by reaching maximum output voltage is plotted in the torque speed domain.

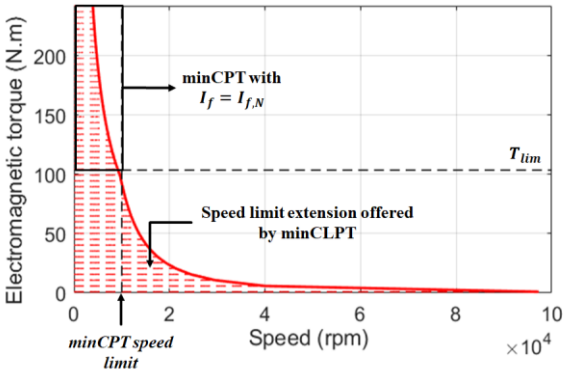

Fig. 8 minCLPT speed limit trajectory in the torque – speed domain

Comparing results in Fig. 8 to those in Fig. 4 show that the EESM field current inclusion in the control algorithm does indeed extend speed limits of conventional MTPA strategies. Torque references below T_{lim} remain reachable within the minCLPT optimization scheme for speed targets that would have required the migration to flux weakening algorithms if the machine was driven by MTPA techniques. It is also

interesting to see that theoretically, at low torque setpoints, speed limits could extend to x20 N_N using the minCLPT algorithm.

V. Energy Efficiency Simulation Results

Now that high speed performances were explored, it remains essential to investigate the novel control scheme energy efficiency improvement, especially copper losses reduction. The first set of results is shown at an operating point inside the minCPT limit zone in order to test if copper losses are reduced at normal operating conditions outside flux weakening area. Point A coordinates in Fig. 5 is chosen as input to the minCLPT algorithm with an objective to investigate copper losses using the latter optimization scheme and the corresponding current references and losses results for both methods are shown in Fig. 9.

Comparing the results in Fig. 9 to those shown in Fig. 5 for point A, concludes that even in optimal minCPT work area, the novel minCLPT algorithm brings better copper losses results as 21.5% less losses are seen (1800 W versus 1400 W). This is mainly caused by the fact that rotor resistance R_f in EESMs are much bigger than the stator one, so keeping the field current at rated values considerably increases field coil copper losses, consequently reducing the drivetrain global efficiency. Although the main minCLPT qualities are found inside conventional flux weakening regions, but it is also interesting to see added value in normal operating conditions areas.

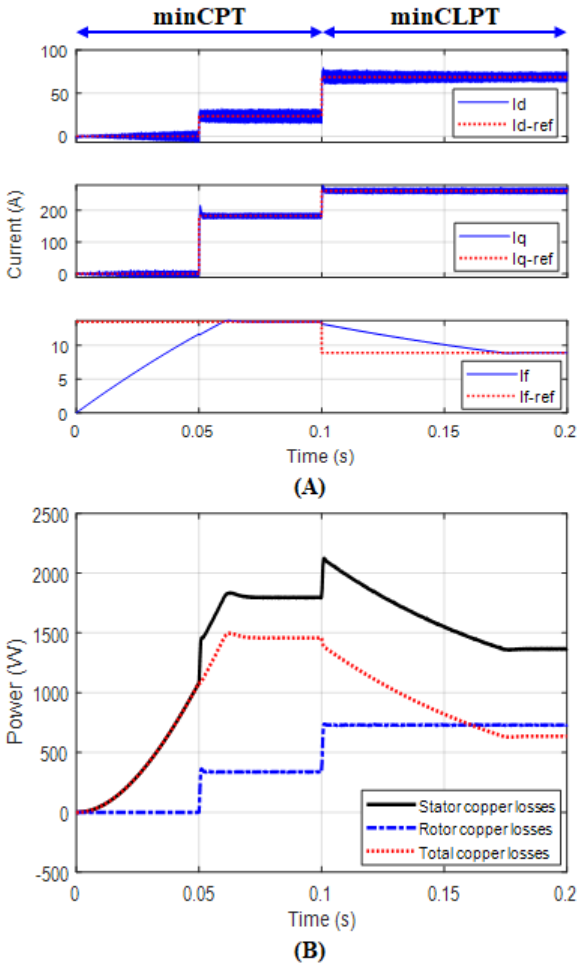

Fig. 9 minCPT and minCLPT resulting currents (A) and copper losses (B) for a step torque from 0 to 50 N.m at 7000 rpm (A operating point)

The next set of results will investigate the major benefits offered by minCLPT algorithm, which consist of efficient operation at high speed setpoints that were unreachable by conventional MTPA strategies and normally required non-efficient flux weakening algorithms. C operating point (25.5 N.m – 15000 rpm) is chosen inside flux weakening region in Fig. 10 where the minCPT algorithm was implemented at constant rated field current and the corresponding current references as well as copper losses are shown on the same plot.

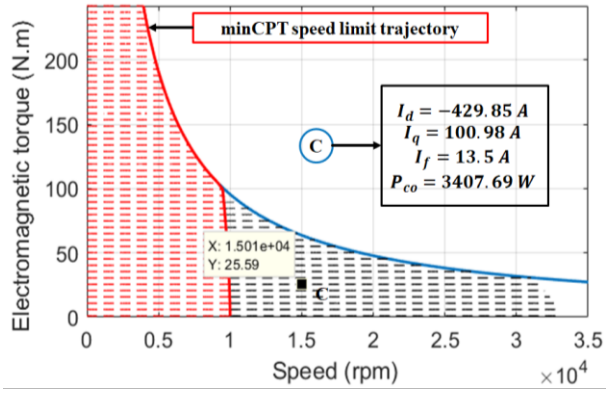

Fig. 10 Current references and copper losses results of a high-speed operating point inside flux weakening area

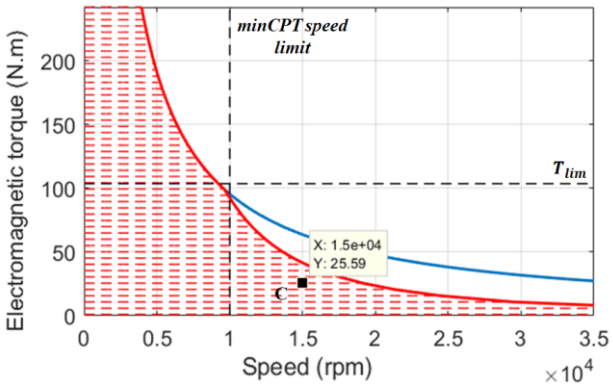

Fig. 11 High-speed operating point marked inside the minCLPT working area

The same high-speed operating point that was only reachable using conventional flux-weakening algorithms (Fig. 10) is henceforth found within the minCLPT limits as shown in Fig. 11, where the minCLPT working area is drawn in the torque – speed domain. The excitation current inclusion in the optimization control algorithm allows both field-weakening and optimization features, since the high-speed operating point is normally driven using the minCLPT control algorithm without having to use negative d-axis currents. The currents and copper losses results at C operating point using minCLPT algorithm are shown in Fig. 12.

Results in Fig. 12 indeed meet the expectations, since the high-speed operating point is reached with much lower losses. Flux weakening algorithms outside conventional MTPA limits generated approximately 3400 Watts of copper losses to drive the machine at C operating point (Fig. 10) whereas the minCLPT algorithm generated around 79% less losses, estimated at 700 Watts. These results would be further explored and the method will be implemented on an experimental setup with the possibility of adding more variables into the equation such as machine parameter

variations, magnetic saturation and other drive train loss elements which algebraic formulations can be found in [9].

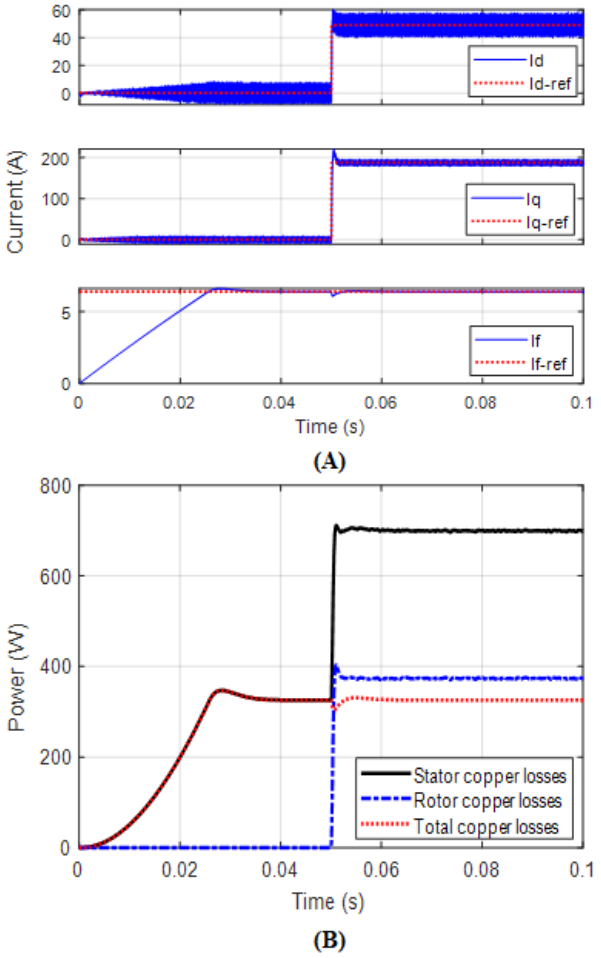

Fig. 12 minCLPT resulting currents (A) and copper losses (B) for a step torque from 0 to 25.6 N.m at 15000 rpm (C operating point)

VI. Conclusion

In this paper, a novel optimization control algorithm is implemented on an EESM using its field current as additional degree of freedom for an efficient torque control, especially in high-speed region. The Lagrange multiplier mathematical technique was used to minimize a non-linear multi variable equation with an aim to drive the machine at any relevant operating point defined by a torque and speed setpoint, with minimum copper losses. The resulting optimal reference currents were stored in lookup tables implemented for usage in the field oriented based current control loop. The EESM was operated under both conventional MTPA methods by keeping its magnetic field constant, and the enhanced optimization method by regulating its field current. Finally, comparative simulation results of both operating modes demonstrated how EESMs field current inclusion in the control algorithm can bring solution to conventional strategies high speed problems. The new control scheme incited future outlooks consisting in implementing the minCLPT resulting reference currents algebraic solutions on a DSP for an experimental setup online optimization scheme with the possibility of including additional constraints (magnetic saturation, parameter variation etc.) into the equation in order to achieve optimal operation.

VII. Appendix

The EESM rated values and parameters are listed in Table 1.

Table 1 EESM rated values and parameters

Symbol	*Meaning*	*Value*
T_N	Rated torque	240 N.m
N_N	Rated speed	4000 rpm
P_N	Rated mech. Power	100 kW
V_{DC}	Rated voltage	400 V
$I_{f,N}$	Rated field current	13.5 A
$I_{S,N}$	Rated stator current	726 A
$V_{f,N}$	Rated rotor voltage	400 V
L_d	d-axis inductance	144 µH
L_q	q-axis inductance	48 µH
M	Mutual inductance	10 mH
L_f	Rotor inductance	1.5 H
R_s	Stator resistance	10 mΩ
R_f	Rotor resistance	8 Ω
p	Pole pair number	2

VIII. References

[1] Yasser A Alamoudi, Azzeddine Ferrah, Raghu Panduranga, Ahmed Althobaiti, F Mulolani. *State-of-the Art Electrical Machines for Modern Electric Vehicles.* 2019 Advances in Science and Engineering Technology International Conferences (ASET), Dubai, 2019.

[2] L.R. Huang, Z.Q. Zhu, W.Q. Chu. *Optimization of electrically excited synchronous machine for electrical vehicle applications.* 8th IET International Conference on Power Electronics, Machines and Drives (PEMD 2016), Glasgow, UK, 2016.

[3] Thomas M. Jahns, Gerald B. Kliman, Thomas W. Neumann. *Interior Permanent-Magnet Synchronou s Motors for Adjustable-Speed Drives*. IEEE transactions on industry applications, Vol. IA-22, n° 2, July/August 1986.

[4] Moritz Märgner, Wilhelm Hackmann. *Control challenges of an externally excited synchronous machine in an automotive traction drive application.* 2010 Emobility - Electrical Power Train, Leipzig, Germany, 2010.

[5] Mohammad Eydi, Mojtaba Ayaz Khoshhava and Hossein Abootorabi Zarchi. *Robust Maximum Torque per Ampere Strategy for Permanent Magnet Synchronous Motor Based on PI-Sliding Mode Controller.* 2019 10th International Power Electronics, Drive Systems and Technologies Conference (PEDSTC), Shiraz, Iran.

[6] Quoc Khanh Nguyen, Matthias Petrich, Jorg Roth-Stielow. *Implementation of the MTPA and MTPV control with online parameter identification for a high speed IPMSM used as traction drive.* 2014 International Power Electronics Conference (IPEC-Hiroshima 2014 - ECCE ASIA), Hiroshima, Japan.

[7] Wenqing Huang, Youtong Zhang, Xingchun Zhang, Guan Sun. *Accurate Torque Control of Interior Permanent Magnet Synchronous Machine.* IEEE transactions on energy conversion, Vol. 29, NO. 1, March 2014.

[8] Quoc Khanh Nguyen, Johannes Schuster, Jörg Roth-Stielow. *Energy Optimal Control of an Electrically Excited Synchronous Motor used as Traction Drive*. 9th International Conference on Power Electronics-ECCE Asia, June 1 - 5, 2015 / 63 Convention Center, Seoul, Korea.

[9] Charbel Zaghrini, Gabriel Khoury, Maurice Fadel, Ragi Ghosn, Flavia Khatounian. *On-line loss and global efficiency simulation tool for electric vehicles applications.* IECON 2021 – 47th Annual Conference of the IEEE Industrial Electronics Society, Toronto, ON, Canada.